PROTEINS: Structure, Function, and Genetics 39:204–211 (2000)

Conversion of Yeast Phosphoglycerate Kinase Into Amyloid-Like Structure

Gregor Damaschun,[1]* Hilde Damaschun,[2] Heinz Fabian,[2] Klaus Gast,[2] Reinhard Kröber,[2] Martin Wieske,[2] and Dietrich Zirwer[2]

[1]*Humboldt-Universität zu Berlin, Institut für Biologie, Berlin, Germany*
[2]*Max-Delbrück-Centrum für Molekulare Medizin, Berlin, Germany*

ABSTRACT **Yeast phosphoglycerate kinase is a structurally well-characterized enzyme consisting of 415 amino acids without disulfide bonds. Anion-induced refolding from its acid-unfolded state gives rise to the formation of worm-like amyloid fibrils with a persistence length of 73 nm. Electron microscopy and small-angle X-ray scattering data indicate that the fibrils have an elliptical cross-section with dimensions of 10.2 nm × 5.1 nm. About half of all amino acids are organized in form of cross-β structure which gives rise to typical infrared spectra, X-ray diffraction and yellow-green birefringence after Congo red staining. The kinetics of amyloid formation, monitored by infrared spectroscopy, dynamic light scattering and X-ray scattering, was found to be strongly dependent on protein concentration. The infrared data indicate that the formation of cross-β structure practically comes to an end already after some hours, whereas the length-growth of the amyloid fibrils, monitored by small-angle X-ray scattering, was not yet completed after 1,300 hours. Proteins 2000;39:204–211.**

Key words: protein folding; misfolding; amyloid; fibrillogenesis; X-ray scattering; dynamic light scattering; electron microscopy; infrared spectroscopy; phosphoglycerate kinase

INTRODUCTION

A number of human diseases, e.g., Alzheimer's disease, Creutzfeldt-Jacob disease and type II diabetes are related to the deposition of protein fibrils causing tissue damage and degeneration.[1–3] The amyloid fibrils develop from abnormal conformational states of normally soluble proteins forming ordered aggregates.[4,5]

Structural properties of amyloid fibrils and the kinetics of fibrillogenesis have been studied by various techniques.[2,6–8] The fibrils are straight and unbranched with diameters in the range between 4 nm and 12 nm, as shown by electron microscopy.[8] Although the precursor proteins forming amyloid fibrils lack sequence homologies and similarities in their native structures, the morphology and structural properties of the fibrils are very alike. X-ray fiber diffraction has demonstrated that all amyloid fibrils exhibit a common cross-β structure.[9] The β-strands and β-sheets are arranged perpendicular and parallel to the fiber axis, respectively. This core structure was derived from the presence of an intense 4.7 Å meridional and a 9–10 Å equatorial reflection in the X-ray fiber diagrams.[2,9]

Lately, evidence is accumulating that also proteins for which no amyloid-related diseases are known can form amyloid fibrils in vitro under appropriate conditions.[5,7,10–13] Guijarro et al.[11] have shown that the SH3 domain of the p85α subunit of bovine phosphatidylinositol 3-kinase forms amyloid fibrils when incubated at pH 2 for several days. Chiti et al.[12] have converted human muscle acylphosphatase into amyloid fibrils by incubation at pH 5.5 in the presence of 25 vol.-% trifluoroethanol. Both proteins are small, consisting of only 90 and 98 amino acid residues, respectively. Konno et al.[14] have reported that even the plant protein monellin from *Dioscoreophyllum cumminsii* can form amyloid-like aggregates.

Recently, studying anion-induced refolding of acid-unfolded yeast phosphoglycerate kinase (PGK) at pH 2, we observed a phenomenon leading to the conclusion that partially folded PGK molecules can also assemble into amyloid-like structures under certain conditions.[13] Yeast PGK is a single-chain α/β protein consisting of 415 amino acids. Its X-ray structure has been determined by Watson et al.[15] The enzyme comprises two domains of about equal size connected by a flexible hinge-region. Under physiological conditions, 35% and 13% of its amino acids are in α-helical and β-sheet conformation, respectively. The protein lacks disulphide bonds. Dialysis from native conditions (20 mM sodium phosphate buffer, pH 6.5) to 10 mM HCl, pH 2 results in complete unfolding of the molecules to an expanded coil state.[16] We tried to refold PGK at pH 2 by adding increasing amounts of either sodium chloride or of the sodium salt of trichloroacetic acid (Na-TCA). The changes in the secondary structure were monitored by circular dichroism spectrometry (CD) in the far ultraviolet. We observed time-dependent changes of the CD spectra at constant salt concentration, if the anion concentrations exceeded critical limits, viz. about 150 mM NaCl or about 9

Grant sponsor: Deutsche Forschungsgemeinschaft; Grant numbers: Da 292/6-2, He 1318/18-2, and Ga 175/12-1; Grant sponsor: Fonds der Chemischen Industrie.

Martin Wieske's present address is Fritz-Haber-Institut der Max-Planck-Gesellschaft, Faradayweg 4-6, D-14195 Berlin, Germany.

*Correspondence to: Gregor Damaschun, Max-Delbrück-Centrum für Molekulare Medizin, D-13092 Berlin, PF 740238, Germany. E-mail: gdamasc@mdc-berlin.de

Received 16 September 1999; Accepted 17 December 1999

mM Na-TCA. The CD spectra changed over a period of many hours in such a way that the formation of increasing amounts of β-sheet structure was indicated. However, the samples remained without any perceptible turbidity. This time-dependent process was further investigated by dynamic light scattering (DLS). DLS is very convenient for determining the hydrodynamic effective radius of the protein molecules in solution and any time-dependent changes in the molecular dimensions. Moreover, simultaneous measurement of the total scattered intensity permits to decide whether the changes are due to changing dimensions of the single molecules or to association and/or dissociation processes.[17] Starting with freshly prepared samples of PGK at pH 2 containing salt concentrations just about the critical ones, we found that the initially monomeric partially folded molecules assemble into dimers, tetramers, and octamers. The results of our CD and DLS measurements led us to the conclusion that the octamers assemble then into amyloid-like linear structures by intermolecular β-sheet formation.[13] To obtain additional, more detailed information about the morphology and the inner structure of the molecular aggregates as well as about the kinetics of the process, we have employed solution X-ray scattering (SOXS), dynamic light scattering (DLS), electron microscopy (EM), infrared spectrometry (IR) and Congo red staining in the present work.

MATERIALS AND METHODS

Yeast 3-phosphoglycerate kinase (EC 2.7.2.3) was purchased from Boehringer Mannheim GmbH (Germany), the sodium salt of trichloroacetic acid 97% from Sigma-Aldrich (Germany). All other chemicals were of analytical grade.

Preparation of Native PGK

The ammonium sulfate-precipitated protein was pelleted and then dissolved in 20 mM sodium phosphate buffer, pH 6.5, 1 mM EDTA. Insoluble material was removed by centrifugation. The supernatant was exhaustively dialyzed against the same buffer. To check the homogeneity of the preparation, an aliquot was applied to an FPLC-Superose 12 column (Pharmacia LKB Biotechnology, Sweden). We found only one symmetric peak without any indication of aggregated protein.

Preparation of Acid-Unfolded PGK

PGK in 20 mM sodium phosphate buffer, pH 6.5, 1 mM EDTA was exhaustively dialyzed against 10 mM HCl, pH 2.

Anion-Induced States of Acid-Unfolded PGK

PGK in 10 mM HCl, pH2 was mixed with appropriate volumes of concentrated solutions of Na-TCA or NaCl in 10 mM HCl, pH 2.

Protein Concentration

PGK concentrations were determined photometrically using $A^{1\%}_{1cm} = 4.95$ at 280 nm.[18]

X-Ray Scattering

The solution X-ray scattering (SOXS) was measured in the step-scan mode on a transmission X-ray diffractometer equipped with five slit-apertures and using Cu-K_α radiation. Our experience has shown that recording successively the scattering curves of the capillary $i_H(s)$, the solvent $i_{Solv}(s)$ and the protein solution $i_{Sol}(s)$ in this mode is more precise at large scattering angles than using a position-sensitive detector. These three scattering curves are needed to obtain the excess-scattering curve $i(s) = i_{Sol}(s) - (1 - w)i_{Solv}(s) - wi_H(s)$ of the protein in solution.[19] w is the volume concentration of the protein, $s = 4\pi\lambda^{-1}\sin\Theta$, λ is the wavelength of the X-rays and Θ the Bragg angle.

The scattering curves were measured at 256 points in the interval from $s_{min} = 0.21$ nm^{-1} to $s_{max} = 31$ nm^{-1}. Scanning of this range took about 2 h. The scattering curves for the amyloid-containing solution with a protein concentration of 18.3 g/L, the solvent and the capillary were scanned 54, 44, and 44 times, respectively. The scattering curves for natively folded PGK at a concentration of 36.8 g/L, measured for comparison, and for the corresponding solvent were scanned eight times each. The samples were held in Mark capillaries at room temperature.

Desmearing of the scattering curves, calculation of the cross-section scattering curve of the amyloids and determination of the radius of gyration of the cross-section were performed by the program SAXS.[20]

Light Scattering

Measurements of static and dynamic light scattering were performed as described in Damaschun et al.[13] Briefly, after addition of NaCl to acid-unfolded PGK the light scattering measurements were started in the kinetic mode,[13] allowing continuous monitoring of the hydrodynamic Stokes radius R_S and the scattered intensity I_S as characteristics of particle dimensions and particle mass, respectively.

Electron Microscopy

PGK samples were diluted in 10 mM HCl, pH2, 9.09 mM Na-TCA to about 13 mg/L and prepared for electron microscopy using a double carbon film technique and 1% uranyl formate as negative stain.[21] Micrographs were taken with a Zeiss EM 910 operating at 100 kV acceleration voltage and a nominal magnification of 63000×.

Infrared Spectroscopy

Infrared spectra were recorded on a Bruker IFS-66 FT-IR spectrometer equipped with a DTGS detector and continuously purged with dry air. Protein solutions were placed between a pair of CaF_2 windows separated by a pathlength of 6 μm. For proper compensation of H_2O absorption, the solvents were measured in a cell with slightly shorter pathlength. For each sample, 256 interferograms were co-added and Fourier-transformed employing a Happ-Genzel apodisation function to generate a spectrum with a nominal resolution of 4 cm^{-1}. The protein

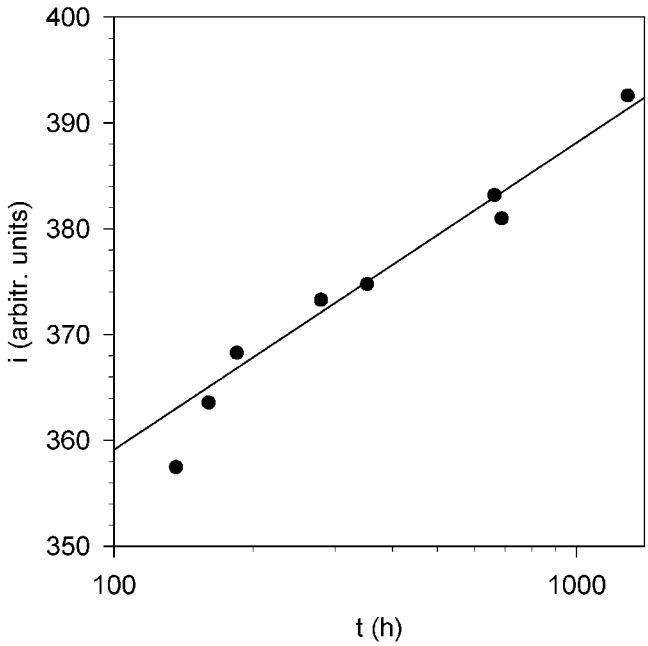

Fig. 1. Time-resolved small-angle X-ray scattering of amyloid PGK at a scattering vector of s = 0.214 nm^{-1} and a concentration of 18.3 g/L. s = $4\pi\lambda^{-1}\sin\theta$.

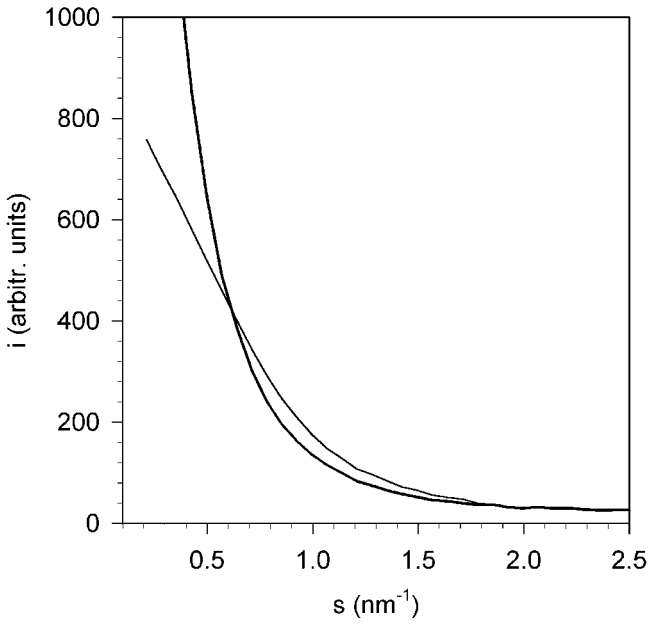

Fig. 2. Slit-smeared solution X-ray scattering curves in the small-angle region of natively folded PGK (thin line) and of the PGK amyloid fibrils (bold line).

spectra were obtained by subtracting the H_2O-buffer spectrum from the spectrum of the protein solution. Minor spectral contributions from residual water vapor were eliminated using a set of water vapor spectra, as described earlier.[22] The final unsmoothed protein spectra were used for further analysis. Band-narrowing by Fourier self-deconvolution was performed using a half-bandwidth of 16 cm^{-1} and a band-narrowing factor k = 1.6. Second-derivative spectra were obtained by Fourier derivation.[23]

Congo Red Staining

Drops of the amyloid- containing solutions on microscope slides were air-dried at 50°C and stained for 20 min in a saturated solution of Congo red in 80% ethanol. After washing with water, 80% ethanol, absolute ethanol, and water, the dried samples were examined microscopically with polarized light regarding birefringence.

RESULTS

X-Ray Scattering

PGK at a concentration of 1.23 g/L in 10 mM HCl, pH 2, 9.09 mM Na-TCA was incubated for 5 days at room temperature and then concentrated in a Centricon 30 (Amicon, USA) to about 20 g/L. The X-ray scattering measurements were started 136 hours after addition of Na-TCA to acid-unfolded PGK.

The small-angle X-ray scattering in the range between s = 0.21 nm^{-1} and s = 1.85 nm^{-1} was strongly time-dependent. Figure 1 shows the time-dependent increase in the scattered intensity at s = 0.214 nm^{-1} up to about 1,300 hours. Figure 2 shows the smeared X-ray scattering curve of this sample compared to that for natively folded PGK. The former curve exhibits a very steep rise in intensity for s < 0.6 nm^{-1}. According to the criteria discussed by Feigin and Svergun, [24]determination of the radius of gyration is unfeasible, because the scattered intensity could be measured only down to s_{min} = 0.21 nm^{-1}.

In contrast to the scattering curve i(s), the cross-section scattering factor $i_c(s) = s\ i(s)$, calculated from the desmeared scattering curve, is independent of time, as shown in Figure 3. The radius of gyration of the cross-section, R_c = 2.87 ± 0.03 nm, can be determined from this cross-section factor (Fig. 3).

In the range s ≥ 1.85 nm^{-1}, the excess-scattering of the sample is independent of time. Figure 4 shows the excess-scattering curve compared to that from natively folded PGK. The former scattering curve exhibits a broad maximum at s = 6 nm^{-1} and a sharp peak at s = 13.3 nm^{-1}. According to the Bragg equation $d = 2\pi s^{-1}$, these values of s correspond to intramolecular distances d = 1.05 nm and d = 0.47 nm. Both values of d are known to be indicative of amyloid structure.

After completion of the scattering measurements, the sample was withdrawn from the capillary, placed on a microscope slide, stained with Congo red after drying and examined under a microscope with polarized light. Amyloid-enriched patches showed bright green-yellow birefringence that was absent in a control experiment with natively folded PGK.

Electron Microscopy

Electron microscopic experiments were performed in parallel to verify that PGK indeed forms amyloid structures, as suggested by earlier CD and DLS studies,[13] the present X-ray scattering measurements and Congo red

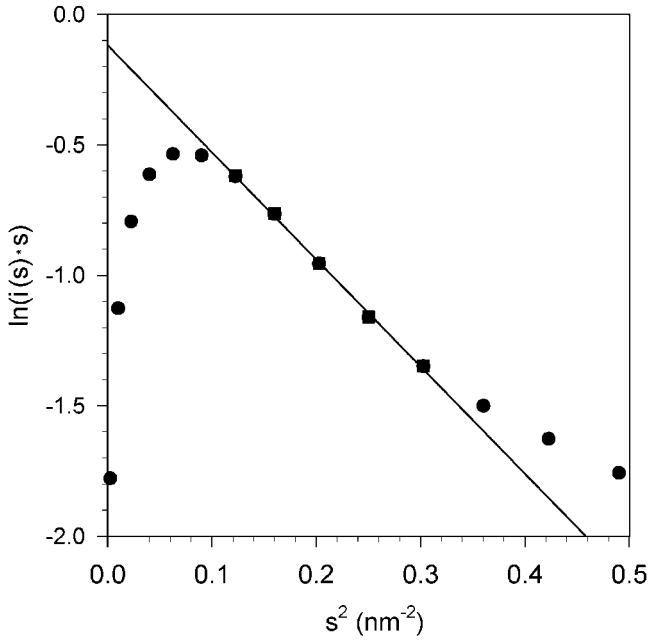

Fig. 3. Guinier plot of the cross-section factor of amyloid PGK. The resulting value for the radius of gyration of the cross-section is R_C = (2.87 ± 0.03) nm.

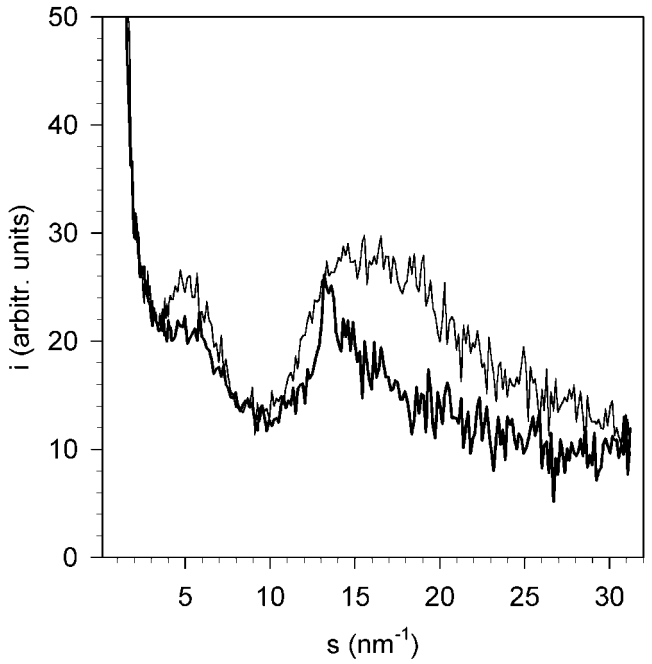

Fig. 4. Solution X-ray scattering curves in the wide-angle region of native PGK (thin line) and of amyloid PGK (bold line) at concentrations of 36.8 g/L and 18.3 g/L, respectively. The maxima at s = 6 nm^{-1} and s = 13.3 nm^{-1} correspond to Bragg distances of 1.05 nm and 0.47 nm, respectively. The profile of the maximum at s = 13.3 nm^{-1} is typical of cross-β structure.

staining. After incubating acid-unfolded PGK at c = 1.3 g/L and room temperature for 24 days in 10 mM HCl, pH 2, 9.09 mM Na-TCA, PGK appears as large worm-like structures with irregular curvature (Fig. 5). The length of these seemingly flexible structures varies in a broad range mainly between 30 and 150 nm, and no branching was observed. The mean diameter is about 9 nm but at certain points the structures are laced to about 4.5 nm (marked by arrowheads in Fig. 5). This indicates a more elliptic or ribbon-like rather than a circular cross-section of the amyloids. So the more slender sides become visible at points where the amyloids are twisted around their longitudinal axes. A regular period between successive twists could not be recognized. Thus electron microscopic data prove the existence of amyloid-like structure of PGK. In control experiments with native PGK, only low molecular mass material was observed (not shown).

Infrared Spectroscopy

Infrared spectroscopy is a sensitive method to indicate the presence of and to probe changes in β-sheet structures. It was employed to characterize structural features of PGK and to monitor the kinetics of its aggregation. The amide I region of the infrared spectrum of the native protein at pH 6.5 is dominated by two major band components at 1,640 and 1,654 cm^{-1} (Fig. 6A). The former reflects the presence of β-sheet structure while the latter testifies a significant amount of α-helical structure known to be present in the native state of PGK. The spectrum of the acid-denatured protein (Fig. 6B) exhibits only a broad, nearly featureless amide I band contour centered at 1,651 cm^{-1} typically of a predominantly unordered protein structure.[25] Unfolding of PGK also leads to spectral changes in the amide II region. The native state is characterized by a relatively sharp band at around 1,547 cm^{-1}, which becomes broader and is centered near 1,549 cm^{-1} for the acid denatured protein. The shoulders at 1,518/1,520 cm^{-1} are due to amino acid side-chain absorptions of tyrosine.[26] The broad feature centered near 1,715 cm^{-1} in the spectrum of PGK at acidic pH arises from the protonated carboxyl groups of glutamic and aspartic acid. The infrared spectra of PGK obtained 10 min after addition of 190.5 mM NaCl to the acid-unfolded protein and almost 6 h later are both clearly different from each other (compare the solid and dashed lines in Figure 6C) and from the spectra of the native and the acid-denatured proteins as well. An α-helical feature at 1,654 cm^{-1} is observed 10 min after addition of salt to the unfolded protein. Interestingly, only a weak band component near 1,635 cm^{-1} which can be associated with β-sheet structures is observed under these conditions. Pronounced features due to β-sheet structures, a strong low-frequency band component at 1,621 cm^{-1} together with a weak high-frequency component near 1,693 cm^{-1}, are seen in the spectrum of PGK obtained 6 h after addition of NaCl (Fig. 6C, solid line). These features are characteristic of aggregated antiparallel β-sheet structures, such as observed in synthetic β-amyloid peptide aggregates[27] or upon thermal aggregation of proteins.[28]

In order to monitor the transition from the partly folded state (10 min after addition of NaCl) to the aggregated state, infrared spectra were collected at discrete times after initiation of the aggregation process. Figure 7 shows

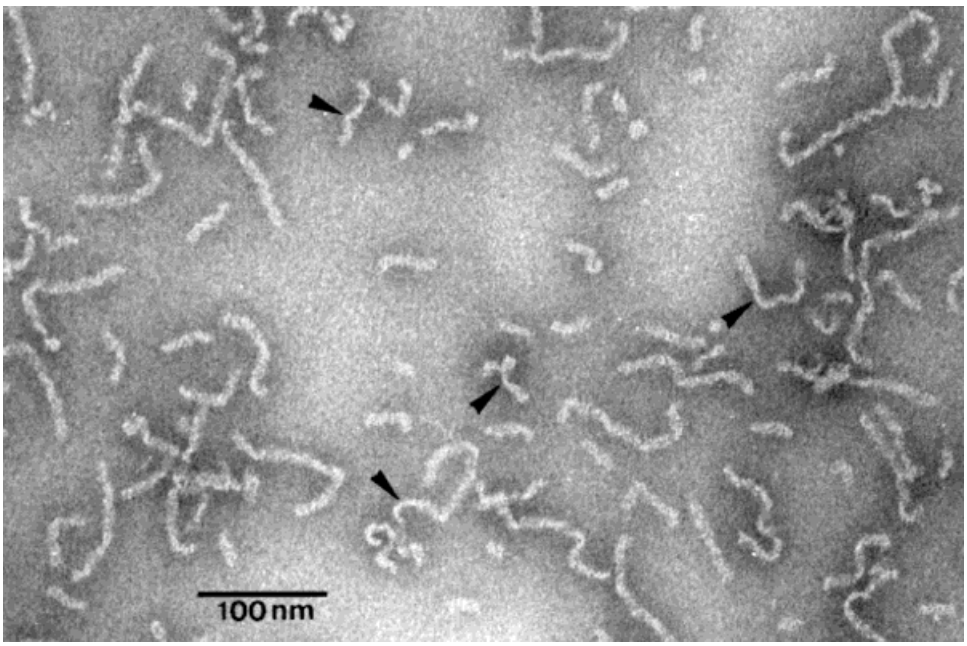

Fig. 5. Analysis of amyloid formation of PGK by electron microscopy. Samples were negatively stained with uranyl formate as described under "Materials and Methods." Arrow heads indicate probable twisting points of the ribbon-like amyloid structures. Magnification 200,000×.

the second-derivatives of these spectra. The α-helical feature at 1,655 cm^{-1} observed 10 min after addition of NaCl practically does not change over the time, suggesting that the formation of α-helical structure is completed within the dead time of the experiment. In contrast, the characteristic features of β-structures at 1,634 and 1,680 cm^{-1} observed 10 min after initiation of the refolding process start to disappear after 30 min, and finally lead to another type of β-sheet structure, as indicated by strong band components at 1,621 and 1,693 cm^{-1}. The spectra obtained between 3 and 6 h were practically identical, indicating that major changes in secondary structure were completed after 3 h under our experimental conditions. It is generally accepted that the weaker the hydrogen bond involving the amide C═O, the smaller is the splitting of the low- and high-frequency β-sheet band components.[28] Based on this empirical approach, the amide I features at 1,634 and 1,680 cm^{-1} point to relatively weak hydrogen-bonding interactions, such as observed in globular proteins.[25] This situation changes drastically as a function of time. The final state observed 3 h after addition of NaCl is characterized by aggregates of β-strands with strong intermolecular hydrogen bonding, as indicated by the β-sheet "marker" bands at 1,621 and 1,693 cm^{-1}. Altogether, the infrared data indicate that the transition from the acid-denatured state to the final state characterized by intermolecular β-sheet aggregates proceeds through at least one intermediate, whose secondary structure contains β-strands involved in an intramolecular-like fashion.

The measurements were repeated at a protein concentration of 6.9 g/L. Figure 8 shows the relative changes in the infrared absorbance at 1,621 cm^{-1} observed between 7 min and 1,000 min. The intensity of this band is proportional to the amount of aggregated antiparallel β-structure (see above).

An aliquot of the preparation was stained with Congo red. The sample showed bright green-yellow birefringence under the polarization microscope.

Dynamic Light Scattering

Figure 8 shows the relative increase in the Stokes radius R_S in dependence on time after initiation of association of the initially monomeric PGK molecules. This experiment was performed under strictly the same conditions (c_{PGK} = 6.9 g/L, c_{NaCl} = 190.5 mM, T = 25°C) as the parallel infrared measurements described in the last section of the previous paragraph. A comparison of the result of the present DLS experiment with that of our earlier measurements at lower protein concentration (1.23 g/L) and in the presence of 9.09 mM Na-TCA (see Fig. 8 in Damaschun et al.[13]) reveals very similar qualitative features of the early stages of the association process. However, the stage of fibril elongation at later times is considerably accelerated in the present experiment.

DISCUSSION AND CONCLUSIONS

The particles developing from anion-induced partially folded states of acid-unfolded PGK exhibit all properties that are characteristic of amyloids. Dried drops of the solution bind Congo red and show the typical green-yellow birefringence when examined under the microscope with polarized light. The electron micrographs reveal unbranched worm-like fibers with cross-section dimensions of about 9 nm × 4.5 nm which are irregularly twisted around their longitudinal axes. To obtain a quantitative

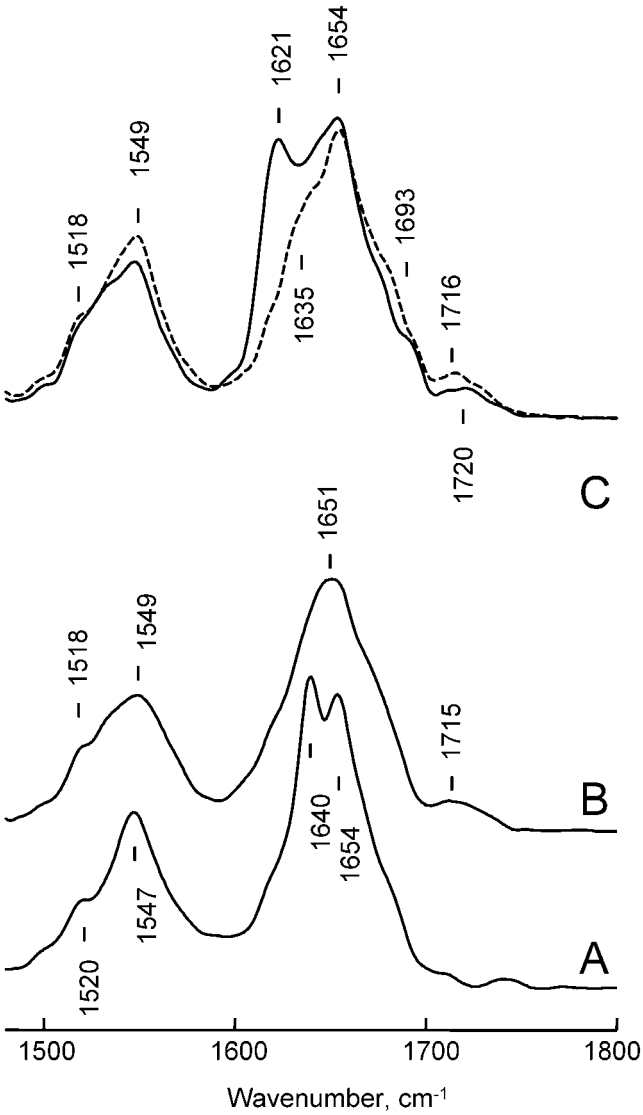

Fig. 6. Infrared spectra of PGK. **(A)** native protein (c = 5.4 g/L) in 20 mM phosphate buffer, pH 6.5; **(B)** acid-unfolded protein (c = 3.8 g/L) in 10 mM HCl, pH 2; **(C)** protein (c = 6.6 g/L) in 10 mM HCl, pH 2 obtained 10 min (dashed line) and 6 hours (solid line) after addition of 190.5 mM NaCl. All spectra are shown after Fourier self-deconvolution performed with the parameters given in "Materials and Methods".

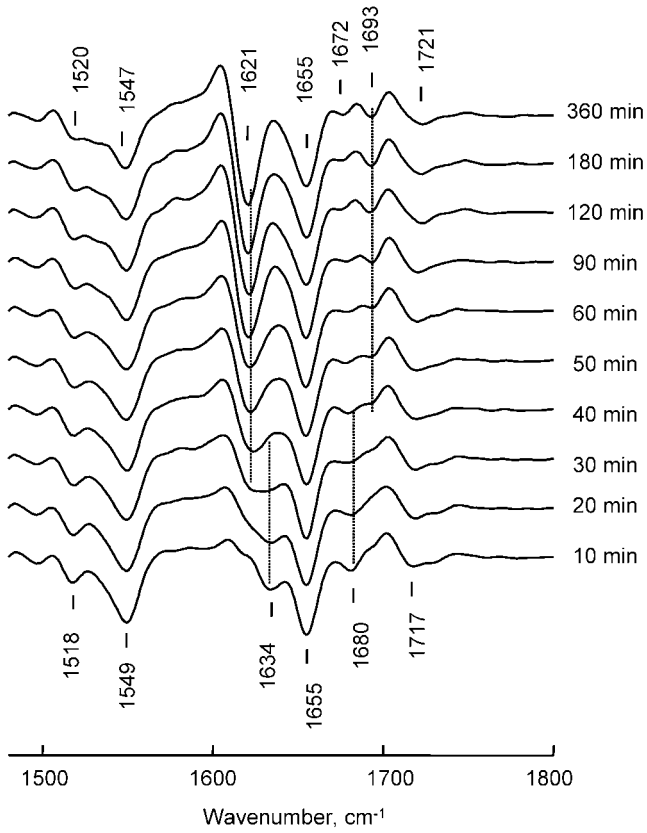

Fig. 7. Second derivative spectra of PGK in 10 mM HCl, pH 2 after addition of 190.5 mM NaCl at the indicated times.

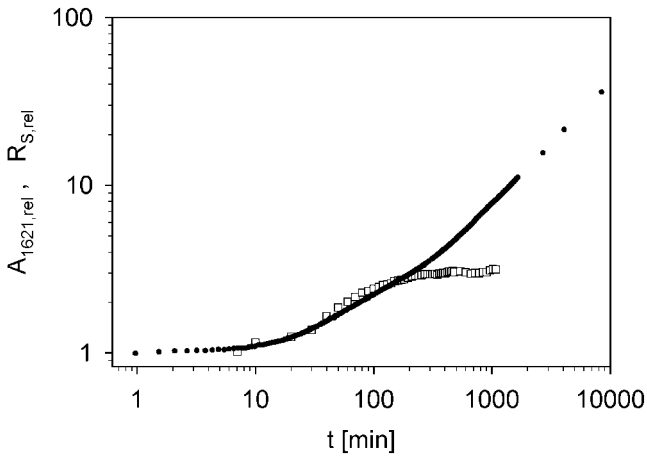

Fig. 8. Comparison of molecular β-sheet formation (□) and particle growth (●) as derived from the infrared "marker" band at 1,621 cm^{-1} and from the Stokes radius. Both quantities are normalized to the initial values (A_{1621} = 0.0059 and R_S = 5.4 nm) after mixing unfolded PGK in 10 mM HCl, pH 2 with an appropriate volume of 4 M NaCl in 10 mM HCl, pH 2, to final concentrations of protein and NaCl of 6.9 g/L and 190.5 mM, respectively.

measure of the fibril curvature, we describe the form of the fibrils by the model of a Kratky-Porod worm-like chain.[29] This model uses as stiffness parameter the persistence length a, defined by the equation

$$a = \lim < \mathbf{R} \cdot \mathbf{u_0} > , \quad L \to \infty$$

where L is the length of the fibril, $\mathbf{R}$ the end-to-end vector, $\mathbf{u_0}$ the unit vector tangent at the contour point zero, and $\langle\ \rangle$ means averaging over many fibrils.

The limit $L \to \infty$ cannot be derived from the electron micrographs. Therefore, we have determined the apparent persistence length $a_{app} \leq a$. We found a value of a_{app} = (73 ± 4) nm. We believe that this method of persistence length determination could be a convenient way for comparing the stiffness of amyloids from different proteins.

Investigating dried amyloid-containing solutions, one cannot exclude the possibility that the mechanism of

β-sheet formation of the amyloids may be driven by interactions at the interface of aqueous solutions and the substrates.[30] This caveat applies also to the usual technique in X-ray diffraction studies to prepare fibers by drying and concomitant stretching of drops of amyloid-containing solutions.[9,31] Therefore, we have attached great importance to techniques by which the properties of amyloids can be investigated in solution, viz. static and dynamic light scattering and CD spectroscopy in Damaschun et al.[13] as well as solution X-ray scattering, dynamic light scattering and IR spectroscopy in the present study. From SOXS in the small-angle range, we have determined the radius of gyration of the cross-section of the fibrils to be $R_C = (2.87 \pm 0.03)$ nm. This value of R_C would correspond to a diameter of 8.12 nm, if the cross-section of the fibrils were circular. However, the electron micrographs suggest rather an elliptic cross-section with an axial ratio about of 2:1 (Fig. 5). Based on the value of R_C, we calculated the corresponding dimensions of a section perpendicular to the long fiber axis to be 10.2 nm × 5.1 nm. This result is in fair agreement with the dimensions derived from the electron micrographs. The minor differences are very probably due to possible fixation effects during preparation of the samples for electron microscopy.

The lower SOXS curve in Figure 4 exhibits two characteristic features in the large-angle region. Comparing the curve with X-ray diffraction patterns from dried amyloids,[9,31] shows that both features are typical of the cross-β structure of amyloids. This applies particularly to the profile of the sharp peak at d = 0.47 nm. The shoulder at d = 1.05 nm, however, appears also in the excess-scattering curve from native PGK (upper curve in Fig. 4).

The infrared spectra (Figs. 6, 7) indicate the formation of intermolecular β-sheet structure, too. Moreover, the IR experiment proves that the formation of the amyloid-like structure does not depend on specific properties of the anions inducing the collapsed state of PGK at pH 2, since NaCl instead of Na-TCA was used in this experiment.

The amyloid-like structures develop from monomeric collapsed folding intermediates with non-native secondary structure (Fig. 6). The IR data suggest that this partially folded state has a significant amount of α-helical and some intramolecular β-structure. Formation of intermolecular β-structure starts later and seems to involve the transformation of some intramolecular into intermolecular antiparallel β-sheet structure.

The kinetics of amyloid formation was monitored by a number of methods yielding different physical parameters, viz. the Stokes radius R_S from DLS, the molar mass from static light scattering , the secondary structure from CD in Damaschun et al.,[13] the secondary structure, particularly β-structure, from IR and the molar mass as well as the radius of gyration of the cross-section from SOXS in the present work. The results from all these methods taken together give interesting insights into the mechanism of formation and growth of the amyloids. Unfortunately, the different methods require very different protein concentrations and also different salts to yield optimum results. For instance, Na-TCA creates some problems in infrared spectroscopy because of the partial overlap of its carboxylate band with the protein amide I band of interest. Therefore, we used NaCl to produce the initial collapsed state of PGK in this case. During a first phase, the initially monomeric folding intermediates form globular particles consisting of ten monomers at most. The growth can be described by the scaling equation $R_S^3 \propto M$, where M is the particle mass (see Figure 10 in Damaschun et al.[13]). The mass fractal dimension of 3 is typical of globular growth. This phase is further characterized by the formation of more and more cross-β structure, as indicated by CD and IR results. The kinetics is strongly dependent on protein concentration. While the formation of intermolecular β-structure comes essentially to an end after approximately 30 hours at c = 1.23 g/L,[13] this stage is reached already after about 3 hours at c = 6.6 g/L, as can be deduced from the IR measurements (Figs. 6 and 7).

Afterwards, the primary molecular clusters grow in one dimension only and assemble into rods or fibrils. This process can be described by the scaling equations $R_S \propto M$ and $L \propto M$, where L is the length of the fibrils. The kinetics conforms to the relation $L \propto M \propto \log t$, where t is the time (Fig. 1). According to the X-ray measurements, the growth of the fibrils was not yet completed when the experiment was terminated at t = 1,300 h. The mechanism of the second growth phase could be explained by assuming that longer fibrils are continually growing at the cost of shorter ones. A similar result was recently obtained by Lansbury and co-workers[32] who studied the in vitro assembly of Aβ amyloid protofibrils and its time dependence using atomic force microscopy. They concluded from a statistical analysis of their data in dependence on incubation time that end-to-end coalescence of smaller protofibrils contributes to protofibril elongation.

To compare the formation of cross-β structure and the growth of the amyloids, we made parallel kinetic measurements of the Stokes radius with DLS and of the increase in cross-β structure with IR spectroscopy. The results are shown in Figure 8. At the protein concentration of c = 6.9 g/L, the increase in cross-β structure essentially comes to an end already after 130 minutes. The elongation of the fibrils, however, continues even after 1,000 minutes. This shows that cross-β structure formation takes place only during the association of monomeric protein to dimeric, tetrameric, and eventually octameric complexes. The octamers assemble then to amyloid fibrils without transforming appreciable parts of the polypeptide chains into more cross-β structure.

The results of our work clearly support the hypothesis that proteins from many different sources can form amyloid-like structures by closely related mechanisms and that this phenomenon is not restricted to a particular disease-related class of proteins. We have shown that also large globular proteins, such as yeast PGK, can be converted from a partially folded into an amyloid-like state. Finally, we want to point out that apart from the 18 amyloidoses with well-known precursor proteins there are further amyloidoses whose precursor proteins are still unknown (for a review see Saeger and Röcken[33]).

ACKNOWLEDGMENTS

We thank Gudrun Lutsch for valuable advice in electron microscopy and Bärbel Lehmann for technical assistance. The Fonds der Chemischen Industrie grant was to G.D.

REFERENCES

1. Pepys MB. Amyloidosis. In: Weatherall DJ, Ledingham JGG, Warell DA, editors. The Oxford textbook of medicine, 3rd edition, Volume 2. Oxford: Oxford University Press; 1996. p 1512–1524.
2. Sunde M, Blake CCF. From the globular to the fibrous state: protein structure and structural conversion in amyloid formation. Quart Rev Biophys 1998;31:1–39.
3. Kelly JW. The environmental dependency of protein folding best explains prion and amyloid diseases. Proc Natl Acad Sci USA 1998;95:930–932.
4. Kelly JW. The alternative conformations of amyloidogenic proteins and their multi-step assembly pathways. Curr Opin Struct Biol 1998;8:101–106.
5. Fink AL. Protein aggregation: folding aggregates, inclusion bodies and amyloid. Fold Des 1998;3:R9–R23.
6. Teplow DB. Structural and kinetic features of amyloid β-protein fibrillogenesis. Amyloid: Int J Exp Clin Invest 1998;5:121–142.
7. Lansbury PT Jr. Evolution of amyloid: what normal protein folding may tell us about fibrillogenesis and disease. Proc Natl Acad Sci USA 1999;96:3342–3344.
8. Sunde M, Blake C. The structure of amyloid fibrils by electron microscopy and X-ray diffraction. Adv Protein Chem 1997;50:123–159.
9. Sunde M, Serpell LC, Bartlam M, Fraser PE, Pepys MB, Blake CCF. Common core structure of amyloid fibrils by synchrotron X-ray diffraction. J Mol Biol 1997;273:729–739.
10. Uversky VN, Segel DJ, Doniach S, Fink AL. Association-induced folding of globular proteins. Proc Natl Acad Sci USA 1998;95:5480–5483.
11. Guijarro JI, Sunde M, Jones JA, Campbell ID, Dobson CM. Amyloid fibril formation by an SH3 domain. Proc Natl Acad Sci USA 1998;95:4224–4228.
12. Chiti F, Webster P, Taddei N, Clark A, Stefani M, Ramponi G, Dobson CM. Designing conditions for in vitro formation of amyloid protofilaments and fibrils. Proc Natl Acad Sci USA 1999;96:3590–3594.
13. Damaschun G, Damaschun H, Gast K, Zirwer D. Proteins can adopt totally different folded conformations. J Mol Biol 1999;291:715–725.
14. Konno T, Murata K, Nagayama K. Amyloid-like aggregates of a plant protein: a case of a sweet-tasting protein, monellin. FEBS Lett 1999;454:122–126.
15. Watson HC, Walker NPC, Shaw PJ et al. Sequence and structure of yeast phosphoglycerate kinase. EMBO J 1982;1:1635–1640.
16. Damaschun G, Damaschun H, Gast K, Zirwer D. Denatured states of yeast phosphoglycerate kinase. Biochemistry (Moscow) 1998;63:308–326.
17. Gast K, Damaschun G, Misselwitz R, Zirwer D. Application of dynamic light scattering to studies of protein folding kinetics. Eur Biophys J 1992;21:357–362.
18. Adams B, Burgess RJ, Pain RH. The folding and mutual interaction of the domains of yeast 3-phosphoglycerate kinase. Eur J Biochem 1985;152:715–720.
19. Damaschun G, Müller JJ, Bielka H. Scattering studies of ribosomes and ribosomal components. Methods Enzymol 1979;59:706–750.
20. Müller JJ, Zalkova TN, Damaschun G, Misselwitz R, Serdyuk IN, Welfle H. Improvements in X-ray scattering data handling and their application to the 5s-rRNA structure determination. Studia Biophysica 1986;112:151–162.
21. Behlke J, Lutsch G, Gaestel M, Bielka H. Supramolecular structure of the recombinant murine small heat shock protein hsp 25. FEBS Lett 1991;288:119–122.
22. Fabian H, Schultz C, Naumann D, Landt O, Hahn U, Saenger W. Secondary structure and temperature-induced unfolding and refolding of ribonuclease T1 in aqueous solution. A Fourier transform infrared spectroscopic study. J Mol Biol 1993;232:967–981.
23. Moffat DJ, Mantsch HH. Fourier resolution enhancement of infrared spectra data. Methods Enzymol 1992;210:192–200.
24. Feigin LA, Svergun DI. Structure analysis by small-angle X-Ray and neutron scattering. New York-London: Plenum Press; 1987. p 68–73.
25. Dong AD, Huang P, Caughey WS. Protein secondary structures in water from second-derivative amide I infrared spectra. Biochemistry 1990;29:3303–3308.
26. Venyaminov SYu, Kalnin NN. Quantitative IR spectrometry of peptide compounds in water (H_2O) solutions. I. Spectral parameters of amino acid residue absorption bands. Biopolymers 1990;30:1243–1257.
27. Fabian H, Choo LP, Szendrei GI, Jackson M, Halliday W, Otvos L, Mantsch HH. Infrared spectroscopic characterization of Alzheimer plaques. Appl Spectros 1993;47:1513–1518.
28. Jackson M, Mantsch HH. The use and misuse of FTIR spectroscopy in the determination of protein structure. Crit Rev Biochem Mol Biol 1995;30:95–120.
29. Kratky O, Porod G. Röntgenuntersuchungen gelöster Fadenmoleküle. Rec Trav Chem 1949;68:1106–1122.
30. Kowalewski T, Holtzman DM. In situ atomic force microscopy study of Alzheimer's β-amyloid peptide on different substrates: New insights into the mechanism of β-sheet formation. Proc Natl Acad Sci USA 1999;96:3688–3693.
31. Inouye H, Domingues FS, Damas AM, Saraiva MJ, Lundgren E, Sandgren O, Kirschner DA. Analysis of x-ray diffraction patterns from amyloid of biopsied vitreous humor and kidney of transthyretin (TTR) Met30 familial amyloidotic polyneuropathy (FAP) patients: axially arrayed TTR monomers constitute the protofilament. Amyloid: Int J Exp Clin Invest 1998;5:163–174.
32. Harper JD, Wong SS, Lieber CM, Lansbury Jr. PT. Assembly of Aβ amyloid protofibrils: an in vitro model for a possible early event in Alzheimer's disease. Biochemistry 1999;38:8972–8980.
33. Saeger W, Röcken C. Amyloid: Mikroskopischer Nachweis, Klassifikation und klinischer Bezug. Pathologe 1998;19:345–354.